SPIE Medical Imaging 2007, 17-22 February 2007, San Diego. SPIE proceedings Vol: 6511: Medical Imaging 2007: Physiology, Function, and Structure from Medical Images, pp. 65110C. DOI: 10.1117/12.709559.

# Quantifying mucosal blood volume fraction from multispectral images of the colon

Ela Claridge[*a], Džena Hidović-Rowe[a], Phillipe Taniere[b] and Tariq Ismail[b]
[a]School of Computer Science and [b]Medical School
The University of Birmingham, Birmingham B15 2TT, U.K.

## ABSTRACT

One of the common physiological changes associated with cancer is the formation of a dense, irregular and leaky network of new blood vessels, which result in the increase of the blood volume fraction (BVF) at the site of a tumour. Such changes are not always obvious through visual inspection using a direct observation, an endoscopic device or colour photography. This paper presents a method for deriving quantitative estimates of BVF of the colon mucosa from multispectral images of the colon. The method has two stages. In the first ("forward") stage a physics-based model of light propagation computes the spectra corresponding to a range of instances of the colon tissue, and in particular the spectral changes resulting from changes in the quantity of blood volume fraction, haemoglobin saturation, the size and density of scattering particles, and the tissue thickness. In the second stage ("model inversion") the spectra obtained from the image data are used to derive the values of the above histological parameters. Parametric maps of the blood contents are created by storing at every pixel the BVF value recovered through the model inversion. In a pilot study multispectral images of ex-vivo samples of the colon were acquired from 8 patients. The samples contained histologically confirmed instances of adenocarcinoma and other pathologies. The parametric maps of BVF showed the significant increase in blood volume fraction (up to 75% above that of the surrounding the normal tissue). A Mann-Whitney test with Bonferroni correction showed that all but one of the differences (a benign neoplastic polyp) are significant ($p<0.00015$).

**Keywords:** Multispectral imaging, colon, colorectal cancer, image analysis, quantitative analysis, blood volume fraction

## 1. BACKGROUND

### 1.1 Introduction

Angiogenesis – the formation of new blood vessels – is one of the common physiological changes associated with cancer. In the colon the first tissue to be affected is mucosa. Standard endoscopy, using RGB imaging, may be ineffective in visualising the resulting changes in colouration. This is because the reddening of the tissue due to the increased blood contents can be visually suppressed through the increased scatter originating from the structural tissues affected by cancer. Multispectral images provide richer information and are more appropriate for representing subtle changes in colouration. Moreover, the use of image interpretation methods based on physics of image formation provides the means for deriving quantitative information from the image data.

The objective of this work was to derive quantitative estimates of the blood contents of the mucosa from multispectral images of the colon, and to determine whether the derived quantities show significant statistical differences between the normal and the cancerous colon tissue.

### 1.2 The structure of the colon

In common with other epithelial tissues the colon has laminar structure, comprising a number of different layers, each with different structure and function [1]. Figure 1 shows schematically the main layers of the colon.

The surface of mucosal layer is made of "fractal" crypts populated with epithelial cells and supported by connective collagenous tissue (lamina propria) and a thin muscle layer. These structures are supplied with blood through a network of capillaries which converge into arterioles and venuoles as they descend deeper into the layer. Submucosa is made of dense connective tissue containing blood and lymphatic vessels. The blood vessels are much larger in this layer than those in mucosa and hence carry a larger blood volume. Muscularis externa is made of smooth muscle layers which are

[*] E.Claridge@cs.bham.ac.uk

also supplied with blood. Serosa, the outermost layer of the colon, is a membrane enclosing the muscularis externa. It contains large blood vessels and lymphatic vessels.

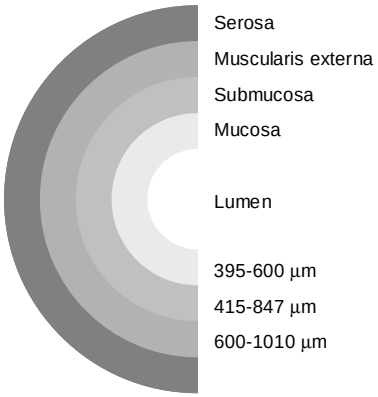


Fig. 1. The main layers of the colon. Starting from the inside of the colon (lumen) and progressing towards the outer surface of the colon are: mucosa, submucosa, muscularis externa and serosa. The numbers to the right show typical thickness of the layers.

### 1.3 Epithelial tumours and their histology

Tumours (or neoplasms) are abnormal growths which can be either benign of malignant. The most common of these are polyps which grow from the epithelial tissue into the lumen of the colon. Hyperplastic polyps are simply outgrowths of the tissue, not containing any abnormal cells. Neoplastic polyps do contain abnormal cells, however these are confined to the body of the polyp and are not present in the "stalk" which connects the polyp to the colon wall. Neoplastic polyps may, in time, develop into cancers. The most diagnostically important neoplastic polyp is adenoma because most colon carcinomas (malignant tumours) arise from adenomas.

The most common type of colon cancer is adenocarcinoma, accounting for around 95% of all colorectal cancers. These cancers develop slowly, causing at first precancerous changes in the mucosa. Only when the cancerous cells invade the lamina propria is the tumour considered to be an invasive carcinoma. In time it penetrates the mucosal muscle layer and reaches the submucosa. Metastatic material may then be carried to other parts of the body via the blood or the lymphatic system.

The growth of a cancer changes the tissue architecture and its histology. In particular, it affects blood vessels which increase in size and density and their network becomes disorganised. The microvasculature of malignant tumours is characterised by the increase of microvessels at the periphery of the mass and the loss of microvessels in its centre. This latter can sometimes lead to necrosis (the death of cells) in the central part of a large or rapidly growing tumour. Other histological changes include the enlargement and hypochromatisms of the mucosal cells, changes in collagen contents, organisation and thickness, and degree of oxygen saturation. This paper will focus on the changes in the blood supply.

### 1.4 Blood volume fraction

The blood content of tissue is an important diagnostic factor, not only for the colon [2] but also for the skin, retina and other epithelial tissues. One way of quantifying the blood content is to compute a fraction of a tissue volume occupied by blood. This will be referred to as the blood volume fraction (BVF). This quantity was derived from the results reported by Skinner et al [2][3] who estimated the volume fraction of blood vessels in colon samples seen in electron microscopy images. By subtracting the volume of the vessel walls this yielded the blood volume fraction, which was found to range between 1% and 10% across different sectors of the colon.

### 1.5 Light propagation through the colon

This work uses image interpretation methods based on the physics of image formation as the means for deriving quantitative information from the imaged data. It is therefore necessary to understand the basic mechanisms by which the spectral composition of light is changed by colon tissue. The two key contributors are light absorption and scatter.

Absorption is a process by which certain wavelengths of light are differentially attenuated by tissue pigments. The main absorbers are pigments such as haemoglobin, oxy-haemoglobin, melanin, etc. The characteristic absorption of a given

pigment can be described by its absorption coefficient, $\mu_a$, which is amount of light absorbed per unit of distance as a function of wavelength, $\lambda$. Figure 2 shows the molar absorption coefficients for haemoglobin and oxy-haemoglobin. A well-known Beer-Lambert law shows the attenuation of incident light $I_0$ by the thickness $b$ of an absorber characterised by $\mu_a$.

$$I = I_0 \, e^{-\mu_a b} \tag{1}$$

Scattering is a process by which photons are deflected from their paths by collision with scattering particles. For scatter to occur the particles must have different refractive index than that of their surrounding medium. Analogously to absorption, the scattering properties of a given material can be characterised by a wavelength-dependent scattering coefficient, $\mu_s$. In the visible range, scattering coefficient decreases as the function of the wavelength.

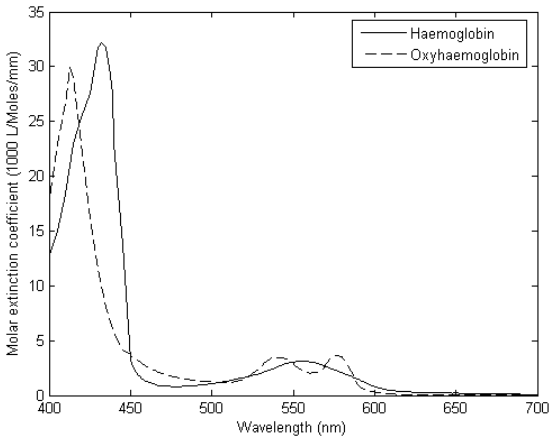


Fig. 2. Molar extinction coefficient for haemoglobin and oxy-haemoglobin.

These two processes are responsible for the changes in the spectral composition of light emerging from the colon. A detailed analysis and modelling of the light propagation through the colon has been described elsewhere [4]. In brief, the incident light is first scattered by epithelial cells, collagen fibres and organelles in the mucosa, and absorbed by oxy- and deoxygenated blood present in mucosal capillaries. A small fraction of light is backscattered at the boundary between the mucosa and submucosa, but most of it enters the submucosa. There, the light is strongly scattered forward by large collagen fibres and strongly absorbed by blood (both oxy- and deoxygenated) present in large submucosal vessels. The non-absorbed light enters the muscle layer where it is further forward-scattered, with the result that very little of it emerges back from the surface. Thus the light which interacted with the constituents of the mucosa, submucosa and the smooth muscle layer is most important for the understanding of the relationship between the colon structure and its spectral reflectance.

## 2. METHODOLOGY

### 2.1 Overview

Our method for deriving quantitative estimates of BVF of the mucosal layer from multispectral images of the colon has two stages. In the first ("forward") stage a physics-based model of light propagation computes the spectra corresponding to a range of instances of the colon tissue, and in particular the spectral changes resulting from changes in the quantity of blood volume fraction, haemoglobin saturation, the size and density of scattering particles, and the tissue thickness. In the second stage ("model inversion") the spectra obtained from the image data are used to derive the values of the above histological parameters and present them in the form of parametric maps.

### 2.2 Forward modelling

As the first step we construct a forward model which predicts reflectance spectra associated with specific instances of colon tissue. The model uses a Monte Carlo simulation [5] of photon propagation through a tissue, which is one of the

possible implementations of the solution to the radiative transport equation [6][7]. It is a probabilistic method in which the passage of a large number of photons through the tissue is simulated. The rules governing the propagation depend on the optical properties of the tissue, such as its scattering and absorption coefficients, refractive index, size and density of scatterers etc. The blood volume fraction is related to these parameters through the equation (2) [8][9][10]

$$\mu_a(\lambda) = V_{Hb} \cdot ln10 \cdot c_{Hb} \cdot (\alpha\, \varepsilon_{HbO2}(\lambda) + (1 - \alpha)\, \varepsilon_{Hb}(\lambda)) \qquad (2)$$

where $V_{Hb}$ is the volume fraction of blood, $c_{Hb}$ is the concentration of haemoglobin per litre of blood, $\alpha$ is the haemoglobin saturation, and $\varepsilon_{HbO2}$ and $\varepsilon_{Hb}$ are the molar extinctions of oxy- and deoxy-haemoglobin; $\lambda$ denotes the wavelength.

The model simulates photon propagation through the three main layers of the colon tissue: mucosa, submucosa and smooth muscle. The optical properties of each layer are characterised by a number of *generic* parameters which are *constant* for a given layer, namely the absorption coefficients and the scattering coefficients as a function of wavelength. From the point of view of our analysis, however, the most important are *variable* parameters which characterise *specific instances* of the tissue. In our model these include blood volume fraction, haemoglobin saturation, the size of scattering particles, their density and the layer thickness. These parameters are varied across their entire physiological ranges to create a cross-reference between their values and the reflectance spectra. The outline of the generic algorithm (see [11]) is as follows:

```
given
 incident light I0
 the number and the order of distinct optical layers
 absorption and scattering coefficients for all the components
for all values of variable parameter p1
 for all values of variable parameter p2
  . . .
    for all values of variable parameter pK
      compute Reflectance_Spectrum [r1,...rM] = Light_Interaction_Model(I0, p1, …, pK)
```

Other parameters, representing the submucosa and the muscle layer, are also represented, but as a constant since our analysis showed that they make constant contribution to the shape of the remitted spectrum [4].

The model spectra are computed for 33 wavelengths in the range of visible light from 450nm to 700 nm. The specific wavelengths were chosen to represent the entire spectrum with high accuracy. It can be observed in figure 3 that the curved section of the spectrum are represented by more points than the linear parts. The model spectra were validated by comparison with the experimental data acquired in vivo. The full details of the modelling and the validation are given in [4].

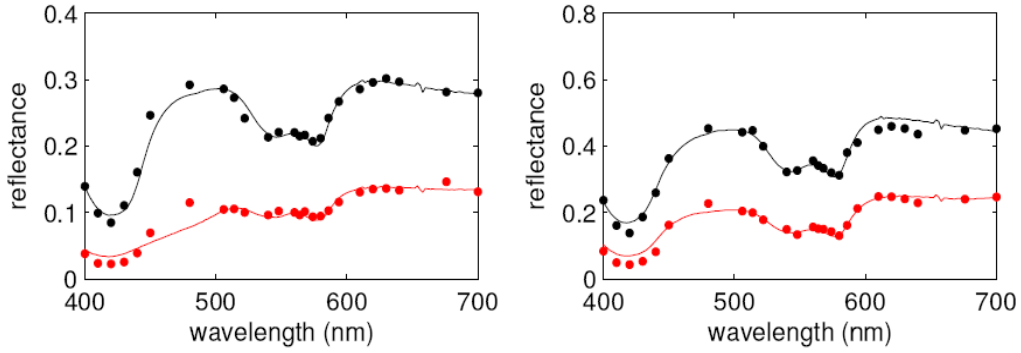


Fig. 3. Example of measured spectra [12] (solid line) and corresponding modelled spectra (disks). Spectra of the normal tissue are shown in black, and of the cancerous tissue from the same patient are shown in red (grey in a monochrome reproduction).

Plots in figure 4(a) and 4(b) shows the families of spectra which demonstrate the variability of spectral reflectance resulting from changes in blood volume fraction in mucosa and (for comparison) the haemoglobin saturation in mucosa. Similar analysis of spectral variability was performed for a range of sizes of scattering particles and their volume fraction in mucosa, the thickness of mucosa, BVF in submucosa, size of collagen fibres in submucosa and thickness of submucosa (see [4]).

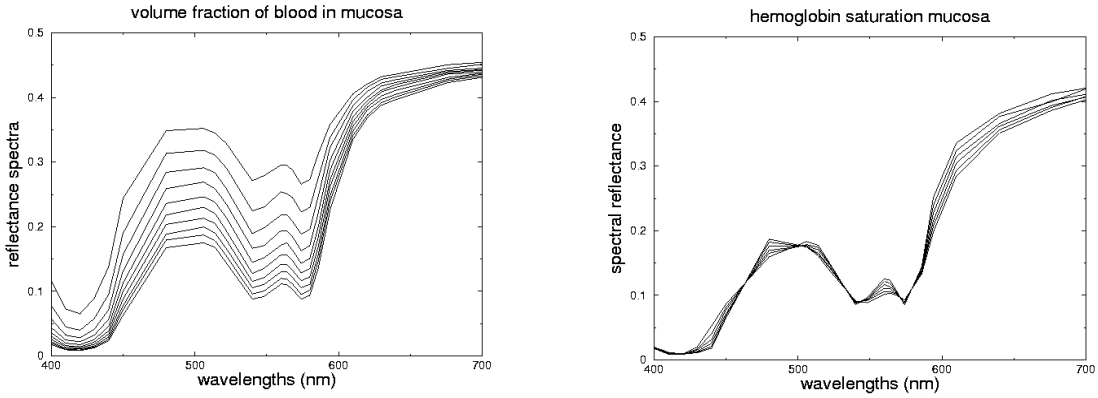


(a) (b)

Fig. 4. Variability of spectral reflectance as a function of wavelength and of varying (a) the BVF in mucosa; and (b) haemoglobin saturation in mucosa. All the remaining parameters (the size of scattering particles, their density and the layer thickness in mucosa, and blood volume fraction, haemoglobin saturation, the size of scattering particles, their density and the layer thickness in submucosa) are set to the same value (mean of the respective range) throughout the simulations.

### 2.3 Inversion and construction of parametric maps

The quantitative estimates of the blood volume fraction (BVF) are obtained through "model inversion", i.e. in contrast to the forward model we compute the parameter values from the image spectra. Using optimisation, we derive a set of parameter values such that a spectrum generated from the parameters using the Monte Carlo (MC) simulation provides the best match to the reflectance spectrum obtained from the image (see section 3.3).

Let us denote a tissue reflectance spectrum as a spectral reflectance vector

$$\mathbf{r} = [r_1, r_2, ..., r_M]. \quad (3)$$

Then the parameter vector $\mathbf{p}^i = [p^i_1, p^i_2, ..., p^i_K]$ which generates the reflectance spectrum $\mathbf{r}^i = [r^i_1, r^i_2, ..., r^i_M]$ such that the distance function (4)

$$d(\mathbf{r}, \mathbf{r}^i) = 1/M \, \Sigma_m \, | r_m - r_m^{\,i} | \quad (4)$$

is at minimum over the set all possible model reflectance spectra $\mathbf{r}$, is taken to provide parameters of the spectrum $\mathbf{p}^i$. In other words,

$$\mathbf{p}^i = Light\_Interaction\_Model^{-1} (\mathbf{r}^i) \quad (5)$$

The above minimisation was implemented as an optimisation problem and solved using an Evolutionary Strategy algorithm (ES) [13]. We also used a novel adaptive approximation method to speed up the convergence of ES by taking a two-step approach. In the first step an approximate solution is sought by using a fast approximation to a light propagation model, and specifically a Kubelka-Munk approximation (described in [14]). A more accurate MC algorithm is then employed to seek the final solution. The details of the entire approach are given in [15]. The optimisation could have been implemented using different distance functions and different algorithms, however the above approach considerably speeded up the convergence which otherwise would have been slow because of the relative slowness of MC computations.

The inversion process returns a complete parameter vector, corresponding to values of mucosal BVF, haemoglobin saturation, the size and density of scattering particles, and thickness of the mucosa. Each of these parameters can be

represented in the form of a parametric map. Parametric maps are created by storing at every pixel the value of a respective parameter recovered through the model inversion. In this paper we present results for the BVF.

# 3. EXPERIMENTS

## 3.1 Samples

Multispectral images of ex-vivo samples of the colon were acquired from 8 patients. The patients were undergoing elective surgery following a pre-operative screening for colon cancer which identified the presence of a cancer or a large adenomatous polyp. All the patients gave informed consent for the use of their tissue samples for research purposes. The samples were placed immediately in a fixative and images were obtained within no more than 1 hour from the excision. The samples contained histologically confirmed instances of adenocarcinoma (N=7), necrotic tissue (N=1), neoplastic polyp (N=1), hyperplastic polyp (N=1), adenomateous polyp (N=2) and normal tissue samples (N=12).

## 3.2 Image acquisition

Multispectral data was acquired at 33 wavelengths (see figure 3 for the approximate spectral locations) using a computer controlled LCD filter (VarSpec, C.R.I.) interfaced to a monochrome 12 bpp camera (Retiga Exi, QImaging). The samples were illuminated through 1" and 3" ports of an integrating sphere (ProLite, U.K.) with a halogen light source. All the equipment was photometrically calibrated. A Spectralon reflectance standard (50% reflectance) was imaged immediately after the tissue using the same imaging setup to provide additional calibration data. Exposure times varied across the wavelength range and were chosen to ensure that images do not have under- or over-exposed regions, and their histograms are centred in the middle of the brightness range. Theacquisition times ranged from 70 msec in the blue end of the spectrum to 9 msec in the red.

## 3.3 Post-processing

Each pixel in a multispectral image set can be denoted by an image vector $i = [i_1 \dots i_M]$ where the m-th component of the vector is the image value $i_m$ corresponding to m-th spectral band. This value is a function of the tissue properties, the incident light and the characteristics of the image acquisition system:

$$i_m = \int_{\lambda} R(\lambda) \cdot I_0(\lambda) \cdot q(\lambda) \cdot f_m(\lambda)\, d\lambda \,. \tag{6}$$

*R(λ) is* tissue reflectance at the wavelength $\lambda$ ($R(\lambda_i) = r_i$), $I_0(\lambda)$ is intensity of incident light at wavelength $\lambda$, $q(\lambda)$ is the quantum efficiency of the camera at $\lambda$, and $f_m(\lambda)$ is the spectral response of the *m*-th filter at the wavelength $\lambda$. It can be seen that the image vector **i** depends on the spectral reflectance of the tissue, $R(\lambda)$, as well as on the parameters characterising the imaging system. By deconvolving $i_m$ with $I_0(\lambda)$, $q(\lambda)$ and $f_m(\lambda)$, which are available as a function of wavelength from instrument calibration, the "pure" tissue reflectance spectrum can be recoverd at each point of the multispectral image. The parameter extraction method described in section 2.3 above is applied to these "pure" spectra to derive the histological parameters and record their values in parametric maps.

## 3.4 Statistical analysis

1000 points were selected (smaller number in some small polyps) from each tissue type in the parametric map of the BVF of each sample. A Mann-Whitney test with Bonferroni correction was carried out to determine whether there is a statistical difference between the blood contents in the pathological and the adjacent normal tissue in each sample.

# 4. RESULTS

The parametric maps of the blood volume fraction show distinctly the increased blood contents in the cancerous regions (see Fig. 5 for one of the examples). In all the cases, adenocarcinoma shows the significant increase in blood volume fraction (up to 75% in comparison to the normal tissue; 13% of the entire histological range of values). The blood contents in the necrotic region is lower (as expected) than in the surrounding tissue. All the adenomateous polyps shows a small increase in the blood contents. The plot in Fig. 6. shows the results for all the samples. The Mann-Whitney test shows that all but one differences are significant ($p<0.00015$). The exception (B9(P), $p>0.05$) is a benign neoplastic polyp.

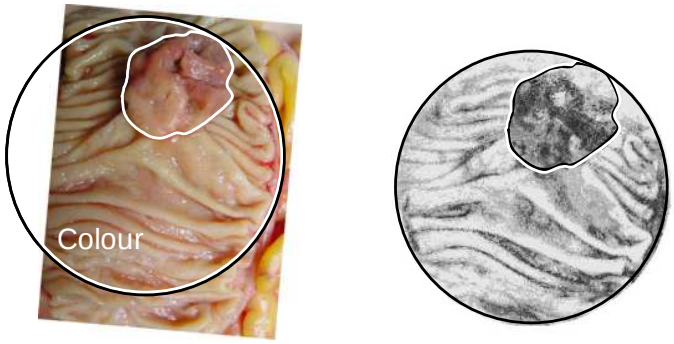


(a) (b)

Fig. 5: (a) Colour image of an excised tissue sample; the cancer outlined in white. (b) Parametric map of the blood volume fraction (darker = more).

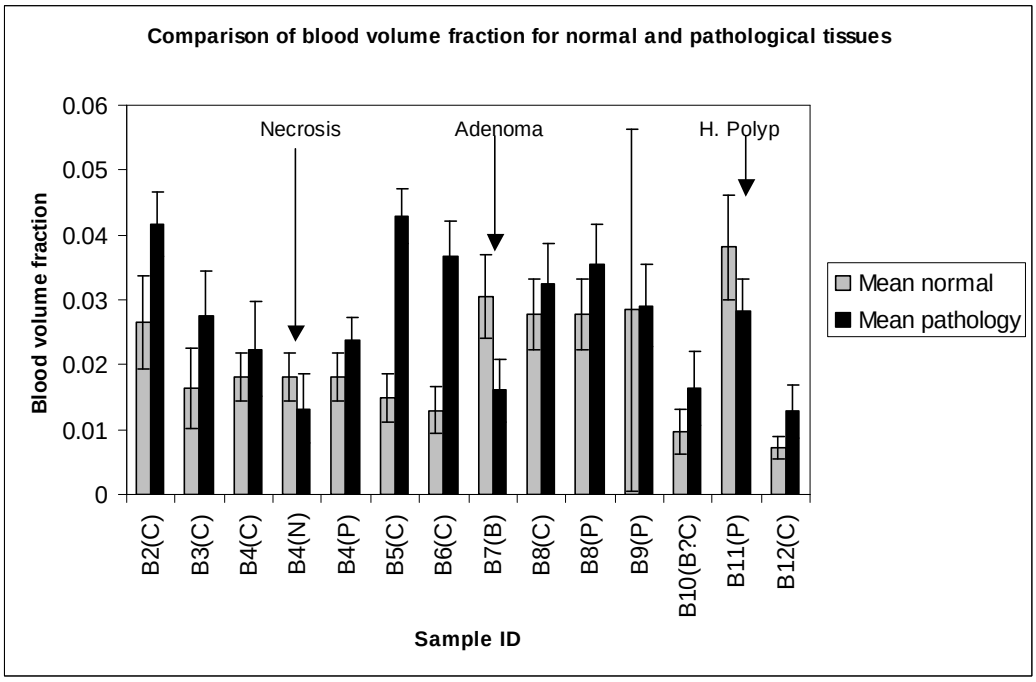


Fig. 6: Comparison of blood volume fraction (BVF) values for normal and pathological colon tissues. The sample number (B<N>) is followed by a pathology code: C = cancer, P = polyp, N = necrosis; B?C = tubulo-villeous adenoma – a tumour which can potentially develop into a cancer B = benign (the Adenoma). The arrows point to the exceptions where BVF is smaller within the pathological region than within the surrounding normal tissue. The total (histologically valid) range of the BVF represented in the model is 0 – 0.1 (0% - 10%).

## 5. CONCLUSIONS

To our knowledge this is the very first time that the values of the blood volume fractions (BVF) for the colon have been computed from multispectral images, and have been demonstrated to show statistically significant differences between normal and the cancerous tissue. Although the reported values are for excised tissue, and therefore are likely to be different than those in the in vivo samples, the differences between the blood volume fraction are likely to be similarly distinct in the living tissue. The BVF values are well within the range estimated by histological and microscopy methods [2], and the nature of differences between the normal and the cancerous tissue are consistent with histology.

Whereas the forward model has been satisfactorily validated [4], we do not yet have such evidence for the parameter recovery method. The results described in this paper are encouraging, but they need to be supported by results from a much larger data set. This is the subject of the ongoing work.

The next major step will be the acquisition and the interpretation of the multispectral colon images in-vivo. The changes to the model will be trivial, as only the parameter ranges will need to be suitably altered to reflect the changes in histology. However, the recovery of the true tissue reflectance spectra ($R(\lambda)$ in Eq. 6) under unknown illumination conditions poses a major challenge. One possible approach has already been developed by our group [16], but it will need to be extended to take account of the colon movement and of the complex illumination in the closed space of the colon. A suitable multispectral imaging endoscopy system is also an issue to be addressed.

The ultimate goal of this research is to enable the clinician to obtain histological information non-invasively, during an *in vivo* endoscopic examination. This may prevent unnecessary biopsies in a growing population of patients undergoing colon cancer screening under a recently introduced programme in U.K. It may also be possible to detect early cancerous changes before they become apparent through a standard endoscopic examination.

## 6. ACKNOWLEDGEMENTS

Kevin Schomacker (MediSpectra, Inc.) is gratefully acknowledged for providing in vivo colon tissue spectra. We thank Dr Nigel Suggett and Dr Emma Hamilton (all from Birmingham University, U.K.) for providing the tissue samples.

## REFERENCES

1. Morson, B. C., *et al. Morson and Dawson's Gastrointestinal Pathology*. Third Ed: Blackwell Scientific Publications, 1990.
2. Skinner, S. A., *et al.* Microvascular Structure of Benign and Malignant-Tumors of the Colon in Humans. *Digestive Diseases and Sciences*. 40:373-384, 1995.
3. Skinner, S. A., Obrien, P. E. The microvascular structure of the normal colon in rats and humans. *Journal of Surgical Research*. 61:482-490, 1996.
4. Hidovic, D., Claridge, E. Modelling and validation of spectral reflectance for the colon. *Physics in Medicine and Biology*. 50:1071-1093, 2005.
5. Prahl, S. A., *et al.* A monte carlo model of light propagation in tissue. In *SPIE Insitute Series*, 102–111, 1989.
6. Arnfield, M. R., *et al.* Optical Propagation in Tissue with Anisotropic Scattering. *Ieee Transactions on Biomedical Engineering*. 35:372-381, 1988.
7. Cheong, W. F., *et al.* A Review of the Optical-Properties of Biological Tissues. *Ieee Journal of Quantum Electronics*. 26:2166-2185, 1990.
8. Jacques, S. L. http://omlc.ogi.edu/news/jan98/skinoptics.html. *Skin Optics. Oregon Medical Laser Centre*, 1998.
9. Prahl, S. A. http://omlc.ogi.edu/spectra/hemoglobin/index.html. *Oregon Medical Laser Centre*, 1999.
10. Meglinski, I. V., Matcher, S. J. Quantitative assessment of skin layers absorption and skin reflectance spectra simulation in the visible and near-infrared spectral regions. *Physiological Measurement*. 23:741-753, 2002.
11. Claridge, E., Preece, S. An inverse method for the recovery of tissue parameters from colour images. In *Information Processing in Medical Imaging (IPMI)*: Springer-Verlag, 306-317, 2003.
12. Ge, Z. F., *et al.* Identification of colonic dysplasia and neoplasia by diffuse reflectance spectroscopy and pattern recognition techniques. *Applied Spectroscopy*. 52:833-839, 1998.
13. Rowe, J. E., Hidovic, D. An evolution strategy using a continuous version of the Gray-code neighbourhood distribution. In: *Genetic and Evolutionary Computation - Gecco 2004, Pt 1, Proceedings*. K. Deb, *et al.* (Eds.), 2004, 725-736.
14. Cotton, S. D., *et al.* Noninvasive skin imaging. In *Information Processing in Medical Imaging*, 501-507, 1997.
15. Hidovic, D., Rowe, J. E. Validating a model of colon colouration using an evolution strategy with adaptive approximations. In: *Genetic and Evolutionary Computation Gecco 2004 , Pt 2, Proceedings*. K. Deb, *et al.* (Eds.), 2004, 1005-1016.
16. Preece, S., *et al.* Model-based parameter recovery from uncalibrated optical images. In *Medical Image Computing and Computer Assisted Intervention (MICCAI 2005)*. Palm Springs, California, 2005.